INL/CON-19-56962-Revision-0

Near Optimality of Matched Filter Detection for Cyclic Prefix Direct Sequence Spread Spectrum

May 2020

Brent A. Kenney, Arslan J Majid, Hussein Moradi, Behrouz Farhang-Boroujeny

Changing the World's Energy Future

Idaho National Laboratory

INL is a U.S. Department of Energy National Laboratory operated by Battelle Energy Alliance, LLC

INL/CON-19-56962-Revision-0

Near Optimality of Matched Filter Detection for Cyclic Prefix Direct Sequence Spread Spectrum

Brent A. Kenney, Arslan J Majid, Hussein Moradi, Behrouz Farhang-Boroujeny

May 2020

Idaho National Laboratory
Idaho Falls, Idaho 83415

http://www.inl.gov

Prepared for the
U.S. Department of Energy
Under DOE Idaho Operations Office
Contract DE-AC07-05ID14517

Near Optimality of Matched Filter Detection for Cyclic Prefix Direct Sequence Spread Spectrum

Brent A. Kenney*, Arslan J. Majid†, Hussein Moradi†, and Behrouz Farhang-Boroujeny*
*Electrical and Computer Engineering Department, University of Utah, Salt Lake City, Utah, USA
†Idaho National Laboratory, Salt Lake City, Utah, USA

***Abstract*—Cyclic Prefix Direct Sequence Spread Spectrum (CP-DSSS) has been presented as a potential solution for ultra-reliable low latency communications (URLLC) and massive machine type communication (mMTC), where the CP-DSSS waveform would operate as a secondary network at the same frequencies as the primary network but at much lower SNR. In this paper, we show that when operating in the low SNR regime, CP-DSSS achieves near optimum performance by using a matched filter (MF) detector at the receiver. Time reversal (TR) precoding at the transmitter is also analyzed. These results also carry forward into multi-antenna scenarios where array gain is preserved. With nearly optimal performance of MF detection, CP-DSSS can be implemented with simple device transceiver structures, reducing per-unit cost for massively deployed networks.**

I. Introduction

Cyclic prefix direct sequence spread spectrum (CP-DSSS) is a waveform designed as a solution to ultra-reliable low latency communications (URLLC) and massive machine type communications (mMTC). The details of the waveform explained in [1] and [2] show how the spreading and despreading operations can be simplified by leveraging the properties of circulant matrices, which result from the use of the cyclic prefix. One promising application of CP-DSSS is as a secondary network waveform, which operates within the same bandwidth as the primary OFDM network but at a lower bit rate and power to keep the interference to the primary network at a negligible level.

This paper derives expressions for calculating the capacity of the CP-DSSS waveform when simple matched filtering (MF) is used at the receiver or time reversal (TR) precoding is used at the transmitter, and compares the results to those of an optimum receiver as reported in [3]. Point-to-point links are the focus of this paper, but the promising results show a path to multi-user topologies using MF detection. For the uplink (UL) scenario, perfect channel state information (CSI) is assumed at the receiver and no CSI is assumed at the transmitter. The downlink (DL) scenario is reversed, where perfect CSI is assumed at the transmitter only. The effects of imperfect CSI will be addressed in future works. Although the DL uses TR precoding without MF at the receiver, it will be shown that the performance is basically identical to the UL case where no precoding is performed and MF detection is used at the receiver.

Matched filtering is an attractive receiver approach because of its computational simplicity. One of the CP-DSSS applications discussed in [3] was a femtocell scenario, where the network density can be dramatically increased by supporting several user terminals in a small geographic area (e.g. 10's of meters), serviced by the femtocell gateway (FGW). One objective of such a scenario is to minimize the complexity of the femtocell terminal in order to reduce cost. When MF detection and TR precoding are performed at the FGW, no CSI is needed at the femtocell terminal, and extremely simple detection is performed. Another major driver to receiver complexity is the forward error control (FEC) coding rate. In order to minimize the computational load, it is desirable to keep these FEC code rates within a practical range (e.g. 0.2 to 0.83 for 5G NR base graph 2, see [4]). CP-DSSS has the ability to reduce symbol rates to operate in this practical FEC rate range with only minor reductions in capacity when in the low SNR regime of a secondary network (e.g. below -10 dB).

The objective of this paper is to show that the capacity of MF detection with CP-DSSS is close to the capacity of an ideal receiver and that TR precoding achieves the same performance. Section II describes aspects of the CP-DSSS waveform that are of particular importance to this performance analysis. Specifically, the methods of precoding, symbol rate reduction, and the corresponding mathematical models for single antenna and multiple antenna operation are discussed. Section III discusses the capacity of CP-DSSS assuming an ideal receiver with either equal power (EP) or TR. In Section IV, we show the derivation of capacity with MF detection and TR precoding for a point-to-point link along with simulated performance values. Finally, Section V contains the concluding remarks.

II. Waveform Summary

The authors in [1] provided details of the CP-DSSS waveform spreading and despreading. A summary of the waveform behavior is presented here for completeness. The spreading sequences used by CP-DSSS are from the family of Zadoff-Chu (ZC) sequences, which have the property of orthogonality between cyclically shifted versions of the same sequence. Let the vector $\mathbf{z}_{(0)}$ represent a ZC sequence of length N scaled to unit power (i.e. $\mathbf{z}_{(0)}^{\mathrm{H}}\mathbf{z}_{(0)} = 1$), where the subscript

This manuscript has in part been authored by Battelle Energy Alliance, LLC under Contract No. DE-AC07-05ID14517 with the U.S. Department of Energy. The United States Government retains and the publisher, by accepting the paper for publication, acknowledges that the United States Government retains a nonexclusive, paid-up, irrevocable, world-wide license to publish or reproduce the published form of this manuscript, or allow others to do so, for United States Government purposes. **STI Number: INL/CON-56962.**

references the size of the cyclic shift. Since each cyclic shift of $\mathbf{z}_{(0)}$ is orthogonal to the other $N-1$ cyclic shifts, there is a potential of modulating N symbols, one on each of the cyclically shifted ZC vectors. We define the spreading matrix $\mathbf{Z}$ as

$$\mathbf{Z} = \begin{bmatrix} \mathbf{z}_{(0)} & \mathbf{z}_{(1)} & \dots & \mathbf{z}_{(N-2)} & \mathbf{z}_{(N-1)} \end{bmatrix}. \quad (1)$$

The corresponding despreading matrix is $\mathbf{Z}^{\mathrm{H}}$, and it can easily be shown that $\mathbf{Z}^{\mathrm{H}}$ is the inverse of $\mathbf{Z}$. Another important property of $\mathbf{Z}$ and $\mathbf{Z}^{\mathrm{H}}$ is that they are circulant matrices; hence, they can be diagonalized by the Discrete Fourier Transform (DFT) matrix, represented as $\boldsymbol{\mathcal{F}}$, and the Inverse DFT (IDFT) matrix, represented as $\boldsymbol{\mathcal{F}}^{-1}$ (i.e. $\mathbf{Z} = \boldsymbol{\mathcal{F}}^{-1}\boldsymbol{\Lambda}_Z\boldsymbol{\mathcal{F}}$ and $\mathbf{Z}^{\mathrm{H}} = \boldsymbol{\mathcal{F}}^{-1}\boldsymbol{\Lambda}_Z^{-1}\boldsymbol{\mathcal{F}}$, where $\boldsymbol{\Lambda}_Z$ is a diagonal matrix). The real advantage of these circulant matrices for spreading and despreading is that they can be implemented in a computationally efficient means by using the Fast Fourier Transform (FFT) and Inverse Fourier Transform (IFFT), resulting in complexity of $\mathcal{O}(N\log N)$ instead of $\mathcal{O}(N^2)$.

The transmitted signal is formed by multiplying the spreading matrix by a vector of N symbols (i.e. $\mathbf{Zs}$) and taking a duplicate of the last N_{cp} samples to be transmitted first as a cyclic prefix (CP). The length of N_{cp} must be greater than or equal to the maximum delay spread of the channel in order to preserve the properties of circular convolution as in the case of OFDM in a 4G LTE or 5G NR context. For the purposes of this paper, we assume that N and N_{cp} are identical to OFDM parameters, where N is the number of OFDM subcarriers. The signal seen by the receiver can now be represented as

$$\mathbf{y} = \mathbf{HZs} + \mathbf{v} \quad (2)$$

after the CP has been removed, where $\mathbf{H}$ is the circulant channel matrix. $\mathbf{H}$ is formed by taking the channel impulse response, $\mathbf{h}$, of length L_h, appending $N - L_h$ zeros to it to form $\mathbf{h}_{(0)}$, and then taking cyclic shifts of $\mathbf{h}_{(0)}$ to create

$$\mathbf{H} = \begin{bmatrix} \mathbf{h}_{(0)} & \mathbf{h}_{(1)} & \dots & \mathbf{h}_{(N-2)} & \mathbf{h}_{(N-1)} \end{bmatrix}, \quad (3)$$

as was done to form $\mathbf{Z}$ in (1).

To despread the received signal, $\mathbf{y}$ is left multiplied by $\mathbf{Z}^{\mathrm{H}}$ to create $\tilde{\mathbf{y}}$. Because $\mathbf{H}$ is circulant, it can also be diagonalized by the DFT matrix such that $\mathbf{Z}^{\mathrm{H}}\mathbf{HZ} = (\boldsymbol{\mathcal{F}}^{-1}\boldsymbol{\Lambda}_Z^{-1}\boldsymbol{\mathcal{F}})(\boldsymbol{\mathcal{F}}^{-1}\boldsymbol{\Lambda}_H\boldsymbol{\mathcal{F}})(\boldsymbol{\mathcal{F}}^{-1}\boldsymbol{\Lambda}_Z\boldsymbol{\mathcal{F}}) = \boldsymbol{\mathcal{F}}^{-1}\boldsymbol{\Lambda}_Z^{-1}\boldsymbol{\Lambda}_H\boldsymbol{\Lambda}_Z\boldsymbol{\mathcal{F}}$. Since diagonal matrices are commutable and $\boldsymbol{\Lambda}_Z^{-1}\boldsymbol{\Lambda}_Z = \mathbf{I}_N$, the despread signal can be represented as

$$\tilde{\mathbf{y}} = \mathbf{Hs} + \tilde{\mathbf{v}}, \quad (4)$$

where $\tilde{\mathbf{v}}$ is the noise vector ($\sim \mathcal{N}(0, \sigma_{\tilde{v}}^2)$) after being left multiplied by $\mathbf{Z}^{\mathrm{H}}$. Since $\mathbf{Z}^{\mathrm{H}}$ is a unitary matrix (i.e. complex orthogonal columns that are unit power), it does not change the noise statistics (i.e. $\sigma_{\tilde{v}}^2 = \sigma_v^2$).

A. Precoding

CP-DSSS has the ability to scale the power on specific frequencies with the same fidelity as OFDM. The power scaling is performed by multiplying the transmitted symbols by a precoding matrix, $\mathbf{G}$, prior to spreading. The resulting received signal with precoding is

$$\tilde{\mathbf{y}} = \mathbf{HGs} + \tilde{\mathbf{v}}, \quad (5)$$

and the effective channel seen by the receiver is now $\mathbf{HG}$. In order to keep the transmitted power constant, there is a constraint that $\mathrm{tr}(\mathbf{G}^{\mathrm{H}}\mathbf{G}) = N$. Another constraint applied to facilitate analysis with precoding in [3] is to make $\mathbf{G}$ circulant. It should be noted that this last constraint does not limit the precoder's ability to scale power on a frequency bin basis.

Two precoding options were discussed in [3]. The first precoder used the water-filling (WF) result, which has been shown to be optimal in terms of capacity for OFDM. It is instructive to note that WF emphasizes strong frequencies of the channel and does not transmit power at frequencies below a calculated threshold. The second precoder used a simple TR filter, which was shown to improve performance over EP. The TR precoder also emphasizes strong frequencies of the channel, but it de-emphasizes weaker frequencies of the channel instead of cutting them off as in WF. The TR precoding technique will be examined in further detail in a later section.

B. Symbol Rate Reduction

Although capacity is generally maximized when N symbols are sent per CP-DSSS frame, there are advantages to reducing the symbol rate. For example, if the capacity calculation shows that the number of bits per symbol is very low (e.g. ≤ 0.1), then a FEC scheme of high complexity must be used to encode the data, resulting in higher transceiver complexity. Reducing the symbol rate allows more power to be transmitted per symbol, while still maintaining the same signal to noise ratio (SNR). Consequently, higher bit to symbol ratios can be used that are within the range of today's FEC schemes (e.g. 0.2 to 0.83 for 5G NR base graph 2, see [4]). Another reason for reducing the symbol rate in CP-DSSS is to spread out the symbols, so that there is less impact from inter-symbol interference (ISI). Both of these reasons will be exploited in a later section.

As described in [3], symbol rate reduction is accomplished by forming an expander matrix, $\mathbf{E}_L$, which is based on the symbol reduction factor, L. The form of $\mathbf{E}_L$ can be described as an identity matrix of dimension N/L (i.e. $\mathbf{I}_{N/L}$) that has been upsampled in the vertical dimension by a factor of L. In other words, after each row of $\mathbf{I}_{N/L}$, $L-1$ rows of zeros are inserted, resulting in an $N \times N/L$ matrix. When symbol reduction and precoding are employed, the received signal takes the form

$$\tilde{\mathbf{y}} = \mathbf{HGE}_L\mathbf{s} + \tilde{\mathbf{v}}, \quad (6)$$

where $\mathbf{s}$ has N/L symbols and each symbol is scaled by $\sqrt{L}$ such that the power per symbol is L times σ_s^2.

C. Multiple Antenna Scenario

Operation with multiple antennas at the base station allows more simultaneous single antenna users to be supported and also reduces the transmitted power level. The system model

shown in (6) can be modified with the following substitutions to facilitate multiple receive antennas in an UL scenario:

$$\tilde{\mathbf{y}} = \begin{bmatrix} \tilde{\mathbf{y}}^{(1)} \\ \tilde{\mathbf{y}}^{(2)} \\ \vdots \\ \tilde{\mathbf{y}}^{(M)} \end{bmatrix}, \mathbf{H} = \begin{bmatrix} \mathbf{H}^{(1)} \\ \mathbf{H}^{(2)} \\ \vdots \\ \mathbf{H}^{(M)} \end{bmatrix}, \tilde{\mathbf{v}} = \begin{bmatrix} \tilde{\mathbf{v}}^{(1)} \\ \tilde{\mathbf{v}}^{(2)} \\ \vdots \\ \tilde{\mathbf{v}}^{(M)} \end{bmatrix}, \quad (7)$$

where M is the number of receive antennas, $\tilde{\mathbf{y}}^{(1)}$ through $\tilde{\mathbf{y}}^{(M)}$ are received signal vectors at the specified antennas, $\mathbf{H}^{(1)}$ through $\mathbf{H}^{(M)}$ are the circulant matrices corresponding to each antenna, and $\tilde{\mathbf{v}}^{(1)}$ through $\tilde{\mathbf{v}}^{(M)}$ are the noise vectors for each antenna. No precoding (i.e. EP) is assumed for the UL scenario.

For the DL scenario, precoding is expected at the transmitter and the following substitutions are made into the system model in (6):

$$\mathbf{H} = \begin{bmatrix} \mathbf{H}^{(1)} & \mathbf{H}^{(2)} & \dots & \mathbf{H}^{(M)} \end{bmatrix}, \mathbf{G} = \begin{bmatrix} \mathbf{G}^{(1)} \\ \mathbf{G}^{(2)} \\ \vdots \\ \mathbf{G}^{(M)} \end{bmatrix}, \quad (8)$$

where the same conventions are used as in (7), and $\mathbf{G}^{(1)}$ through $\mathbf{G}^{(M)}$ are the precoding matrices corresponding to each antenna element.

III. Capacity of an Ideal Receiver

The capacity of an ideal receiver is based on the mutual information of the received signal and the transmitted symbols without applying the limitations of a specific receiver, as was shown in [3]. Using the system model (6) with the results of [3] allows us to express the ideal capacity as

$$C = W \log_2 \left(|\mathbf{I}_N + L \frac{\sigma_s^2}{\sigma_{\tilde{v}}^2} \mathbf{H}\mathbf{G}\mathbf{E}_L \mathbf{E}_L^{\mathrm{H}} \mathbf{G}^{\mathrm{H}} \mathbf{H}^{\mathrm{H}}| \right). \quad (9)$$

The ideal capacity for equal power EP precoding is shown in Fig. 1 for different values of L. This result as well as all of the simulated results in this paper use $N = 2048$ with 130 samples per channel, using a roll-off time constant of 25. The high roll-off time constant was used to show the robust nature of MF detection and TR precoding. The curves represent average capacity taken over 1000 randomly generated channels.

IV. Capacity with MF Detection or TR Precoding

When capacity is calculated with a particular detector at a receiver, the result is expected to be lower than the capacity shown in the previous section. Starting with the most general channel model presented thus far (6), we can substitute the matrix $\mathbf{D}$ for the matrix multiplication $\mathbf{HG}$, where $\mathbf{D}$ represents the channel seen by the receiver. Note that the channel power of $\mathbf{D}$ can be calculated as $\mathrm{tr}(\mathbf{D}^H\mathbf{D}/N) = \mathbf{d}^H\mathbf{d}$, where $\mathbf{d}$ is the first column of $\mathbf{D}$. Since some parts of the spectrum that were pre-emphasized by $\mathbf{G}$ are further emphasized by the channel, $\mathbf{H}$, the resulting channel power can be greater than unity even though the transmit power has been kept fixed by normalizing the precoder matrix $\mathbf{G}$. The SNR referenced in this paper is the ratio of the received signal power without precoding (i.e. $\mathbf{G} = \mathbf{I}_N$) to the noise power of the receiver.

A. Matched Filter Detection

Matched Filter detection is one of the simplest forms of detection, assuming the effective channel (i.e. precoding and channel effects) is known to the receiver. It is also a very effective means of detecting signals at low SNR, as will be seen in this subsection. Matched filtering is convolution by the time-reversed impulse response. As shown earlier, this is performed by a left multiplication of $\mathbf{D}^H$. The reciprocal operation of the expander must also be accounted for in order to arrive at the proper number of received symbols. Hence, the matched filter estimate of the transmitted symbols is given as

$$\hat{\mathbf{s}} = \frac{\mathbf{E}_L^{\mathrm{H}}\mathbf{D}^{\mathrm{H}}}{\mathbf{d}^{\mathrm{H}}\mathbf{d}} \tilde{\mathbf{y}} = \frac{\mathbf{E}_L^{\mathrm{H}}\mathbf{D}^{\mathrm{H}}\mathbf{D}\mathbf{E}_L}{\mathbf{d}^{\mathrm{H}}\mathbf{d}} \mathbf{s} + \frac{\mathbf{E}_L^{\mathrm{H}}\mathbf{D}^{\mathrm{H}}}{\mathbf{d}^{\mathrm{H}}\mathbf{d}} \tilde{\mathbf{v}}, \quad (10)$$

where the divisor, $\mathbf{d}^{\mathrm{H}}\mathbf{d}$, is used to properly scale the symbols.

When the length of the channel $\mathbf{d}$, L_{d}, is less than or equal to L, the signal component of (10) is simply $\mathbf{s}$ because there are no inter-symbol interference (ISI) terms. Here it should be noted that the signal power of each element of $\mathbf{s}$ is $L\sigma_s^2$. Since the number of symbols transmitted is reduced by a factor of L, the increase of signal power per symbol by L maintains a consistent transmitted power and overall SNR.

When $L_{\mathrm{d}} > L$, there are several terms resulting from ISI. Although the length of $\mathbf{d}$ could be as high as N, L_{d} represents the contiguous portion of $\mathbf{d}$ that includes all of its non-zero elements. These ISI terms can be expressed in terms of head and tail portions of the contiguous non-zero (or mostly non-zero) section of $\mathbf{d}$. There will be $2K = 2(\lfloor \frac{L_{\mathrm{d}}-1}{L} \rfloor - 1)$ interference terms that can be defined in terms of K head vectors (i.e. $\mathbf{d}_{\mathrm{h},1}$, $\mathbf{d}_{\mathrm{h},2}$, ..., $\mathbf{d}_{\mathrm{h},K}$) and K tail vectors (i.e. $\mathbf{d}_{\mathrm{t},1}$, $\mathbf{d}_{\mathrm{t},2}$, ..., $\mathbf{d}_{\mathrm{t},K}$. The length of the head and tail vectors are defined by their offset from the diagonal, k. The head vectors are represented by

$$\mathbf{d}_{\mathrm{h},k} = [d_0, d_1, ..., d_{L_{\mathrm{d}}-Lk-2}, d_{L_{\mathrm{d}}-Lk-1}]^{\mathrm{T}}, \quad (11)$$

and the tail vectors are represented by

$$\mathbf{d}_{\mathrm{t},k} = [d_{Lk}, d_{Lk+1}, ..., d_{L_{\mathrm{d}}-2}, d_{L_{\mathrm{d}}-1}]^{\mathrm{T}}. \quad (12)$$

The head and tail vectors are of the same length for a given value of k, getting shorter as k grows larger. After some manipulation, we form the amplitude of the interference terms as

$$\mathbf{r} = \frac{\sqrt{L}}{\mathbf{d}^{\mathrm{H}}\mathbf{d}} \sum_{k=1}^{K} \left(\mathbf{d}_{\mathrm{t},k}^{\mathrm{H}} \mathbf{d}_{\mathrm{h},k} \mathbf{s}_{(k)} + \mathbf{d}_{\mathrm{h},k}^{\mathrm{H}} \mathbf{d}_{\mathrm{t},k} \mathbf{s}_{(-k)} \right) \quad (13)$$

where $\mathbf{s}_{(k)}$ is a circularly shifted version of $\mathbf{s}$ shifted by k places, and $\frac{\mathbf{E}_L^{\mathrm{H}}\mathbf{D}^{\mathrm{H}}\mathbf{D}\mathbf{E}_L}{\mathbf{d}^{\mathrm{H}}\mathbf{d}} \mathbf{s} = \mathbf{s} + \mathbf{r}$. Each of the elements of $\mathbf{r}$ in (13) result in the same variance (i.e. interference power), which is expressed as

$$\sigma_r^2 = 2L\sigma_s^2 \sum_{k=1}^{K} \frac{\mathbf{d}_{\mathrm{t},k}^{\mathrm{H}} \mathbf{d}_{\mathrm{h},k} \mathbf{d}_{\mathrm{h},k}^{\mathrm{H}} \mathbf{d}_{\mathrm{t},k}}{(\mathbf{d}^{\mathrm{H}}\mathbf{d})^2}. \quad (14)$$

Since the noise, $\tilde{\mathbf{v}}$, is also modified by the matched filtering process, we can define a new noise variable as

$$\bar{\mathbf{v}} = \frac{\mathbf{E}_L^{\mathrm{H}}\mathbf{D}^{\mathrm{H}}}{\mathbf{d}^{\mathrm{H}}\mathbf{d}} \tilde{\mathbf{v}}, \quad (15)$$

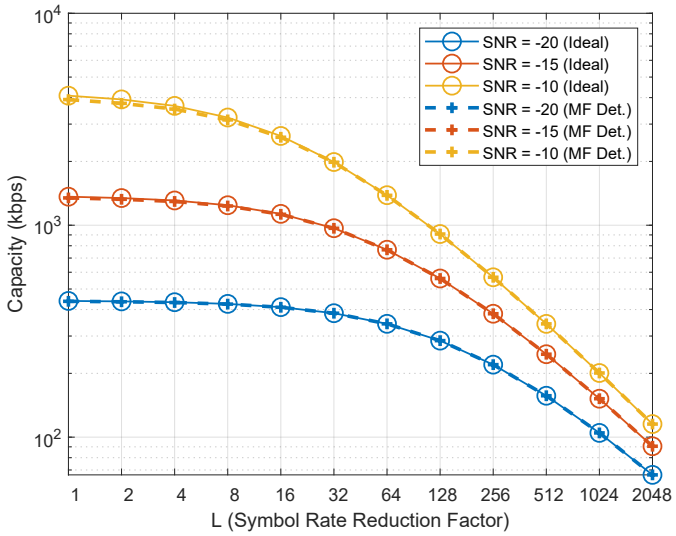

Fig. 1. Capacity with an ideal detector and a MF detector for different symbol rate reduction factors, L. Note that there is negligible difference between the ideal and MF curves for the SNR values shown.

where $\bar{\mathbf{v}}$ is a vector with N/L elements. Each term of $\bar{\mathbf{v}}$ is a weighted sum of the elements of $\tilde{\mathbf{v}}$, where the weights are given by the elements of $\mathbf{d}$ divided by $\mathbf{d}^{\mathrm{H}}\mathbf{d}$. Since, $\tilde{\mathbf{v}}$ is i.i.d. $\sim \mathcal{N}(0, \sigma_{\tilde{v}}^2)$, the variance of $\bar{\mathbf{v}}$ can be calculated by summing the variance of each of the elements resulting in a distribution of $\sim \mathcal{N}(0, \sigma_{\tilde{v}}^2/\mathbf{d}^{\mathrm{H}}\mathbf{d})$, which is independent of the relation of L_{d} to L. The resulting signal to interference plus noise ratio (SINR), ρ_{MF}, can now be expressed as

$$\rho_{\mathrm{MF}} = \frac{L\sigma_s^2}{\sigma_r^2 + \frac{\sigma_{\tilde{v}}^2}{\mathbf{d}^{\mathrm{H}}\mathbf{d}}}. \tag{16}$$

Using the expression for SINR given in (16), we can use Shannon's capacity theorem for each of the symbols transmitted in a frame (i.e. N/L), namely

$$C_{\mathrm{MF}} = \frac{NW}{L}\log_2\left(1 + \rho_{\mathrm{MF}}\right). \tag{17}$$

Fig. 1 shows the MF detection capacity without precoding in relation to the capacity of an ideal receiver. Since CP-DSSS is designed to function as a secondary network at low SNR, the lower SNR values are of particular interest. At the SNR values shown in Fig. 1, the MF performance is nearly optimum. Conventional wisdom would lead one to expect that performance would be worse for $L = 1$ where ISI is highest. However, the noise variance dominates at these low SNRs, so the ISI has little effect. Nevertheless, it may still be advantageous to operate with a higher symbol rate reduction factor so that the coding rate is not extremely low. Fig. 1 shows that there is little capacity penalty for increasing L at low SNR (e.g. -20 dB).

B. Time Reversal Precoding without MF Detection

When the transmitter has CSI but receiver does not, then the transmitter should precode the transmission in order to improve the SINR of the received signal. The receiver will still apply the Hermetian of the expander matrix, $\mathbf{E}_L^{\mathrm{H}}$, to the received signal and also scale it by dividing by the resulting channel power, $\mathbf{h}^{\mathrm{H}}\mathbf{h}$, which can be obtained through a pilot or sounding reference signal. When the precoder is chosen to be a time-reversed (TR) version of the channel impulse response (i.e. $\mathbf{G} = \mathbf{H}^{\mathrm{H}}$), the symbol estimates can be represented as

$$\hat{\mathbf{s}} = \frac{\mathbf{E}_L^{\mathrm{H}}}{\mathbf{h}^{\mathrm{H}}\mathbf{h}}\tilde{\mathbf{y}} = \frac{\mathbf{E}_L^{\mathrm{H}}\mathbf{H}\mathbf{H}^{\mathrm{H}}\mathbf{E}_L}{\mathbf{h}^{\mathrm{H}}\mathbf{h}}\mathbf{s} + \frac{\mathbf{E}_L^{\mathrm{H}}}{\mathbf{h}^{\mathrm{H}}\mathbf{h}}\tilde{\mathbf{v}}. \tag{18}$$

If $\mathbf{H}$ and $\mathbf{H}^{\mathrm{H}}$ where replaced with $\mathbf{D}^{\mathrm{H}}$ and $\mathbf{D}$, respectively, then the channel power could be expressed as $\mathbf{d}^{\mathrm{H}}\mathbf{d}$ instead of $\mathbf{h}^{\mathrm{H}}\mathbf{h}$ without loss of generality. The resulting equation looks much like (10) except that the noise term would be missing the $\mathbf{D}^{\mathrm{H}}$ multiplier. As a result, the variance of the resulting noise equals $\sigma_{\tilde{v}}^2/\left(\mathbf{d}^{\mathrm{H}}\mathbf{d}\right)^2$ instead of $\sigma_{\tilde{v}}^2/\mathbf{d}^{\mathrm{H}}\mathbf{d}$ as before. However, since the channel power is set to be unity for this derivation, the variance is just $\sigma_{\tilde{v}}^2$. Note that when there is no precoding (i.e. equal power case where $\mathbf{D} = \mathbf{H}$) and MF is used at the receiver, the interference value and noise variance are exactly the same as the TR case, resulting in identical performance.

The ideal capacity for a TR precoded signal is much higher than the ideal capacity without precoding, as shown in [3]. If MF detection were used at the receiver, then capacity near the ideal case would be attained. However, this work focuses on the case where CSI is only available on one side of the link. As a result, the capacity with TR precoding but without MF detection is the same as the EP case (no precoding) with MF detection shown in Fig. 1.

C. Multiple Antennas with MF Detection (UL)

Multiple antenna UL operation is best described in a use scenario such as a femtocell, where a single antenna terminal is transmitting to a multi-antenna FGW. In this case, no precoding is applied by the terminal prior to transmission. Each antenna of the FGW receives the signal and applies a matched filter detector. Estimates of the transmitted signals are obtained in the same way as shown in (10), where $\mathbf{D}$ is replaced with the multi-antenna $\mathbf{H}$ matrix that is defined in (7). Since $\mathbf{H}$ is a stacked matrix of M square submatrices, $\mathbf{H}^{\mathrm{H}}\mathbf{H}$ can be represented as a sum of the product of the submatrices (i.e. $\mathbf{H}^{\mathrm{H}}\mathbf{H} = \sum_{m=1}^{M}\mathbf{H}^{(m)\mathrm{H}}\mathbf{H}^{(m)}$). With this observation in mind, (13) can be adapted for multi-antenna operation as

$$\mathbf{r} = \frac{\sqrt{L}\sum_{k=1}^{K}\sum_{m=1}^{M}\left(\alpha_k^{(m)}\mathbf{s}_{(k)} + \alpha_k^{(m)\mathrm{H}}\mathbf{s}_{(-k)}\right)}{\sum_{m=1}^{M}\mathbf{h}^{(m)\mathrm{H}}\mathbf{h}^{(m)}}, \tag{19}$$

where $\alpha_k^{(m)} = \mathbf{h}_{\mathrm{t},k}^{(m)\mathrm{H}}\mathbf{h}_{\mathrm{h},k}^{(m)}$. The interference power can now be calculated in a similar manner as (14) by

$$\sigma_r^2 = \frac{2L\sigma_s^2\sum_{k=1}^{K}|\sum_{m=1}^{M}\alpha_k^{(m)}|^2}{\sum_{m=1}^{M}\mathbf{h}^{(m)\mathrm{H}}\mathbf{h}^{(m)}}. \tag{20}$$

Fig. 2 shows the UL capacity for several FGW array sizes with an ideal detector (solid lines) as well as the capacity when using a MF detector (dashed lines). As was shown for the single antenna case, the MF capacity is virtually indistinguishable from the ideal capacity below -10 dB SNR no matter the size of the array. As a result, CP-DSSS can gain the full advantage of array processing with a MF detector.

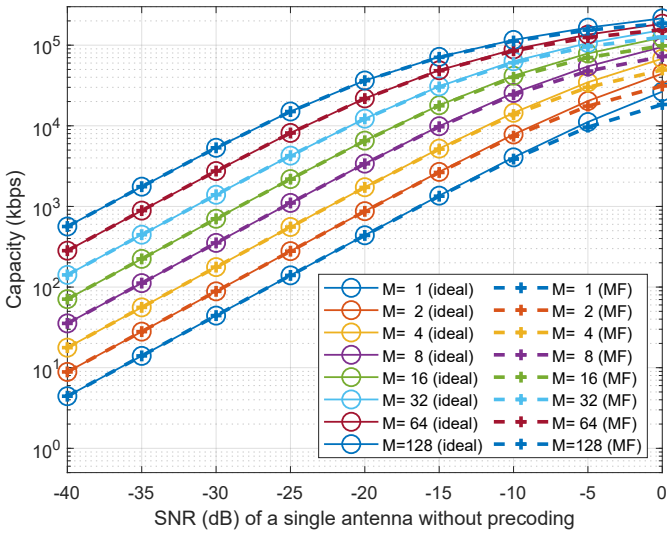

Fig. 2. Capacity with an ideal detector and a MF detector for varying numbers of antennas in an UL scenario. Data is shown for L=1.

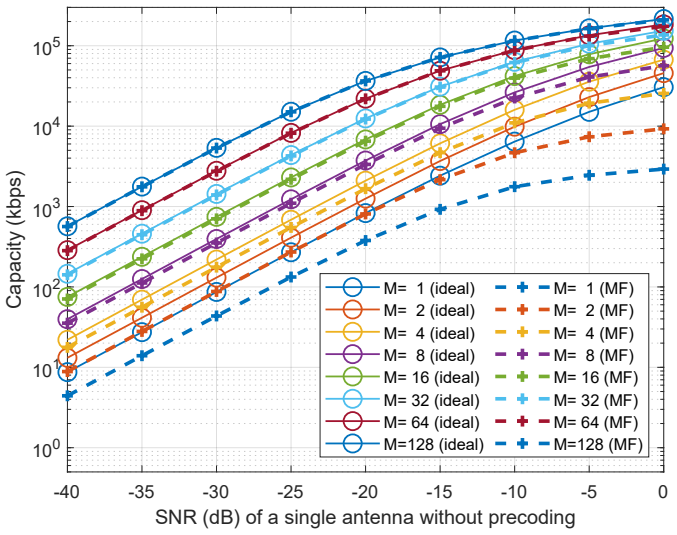

Fig. 3. Capacity with an ideal detector and a MF detector for varying numbers of antennas in a DL scenario. Data is shown for L=1.

D. Multiple Antennas with TR Precoding (DL)

The objective in precoding for the downlink is to maximize the signal at the intended receiver and minimize interference. The downlink model in this paper shows the formulation for a single receiver, but it could be easily extended for a multiple user scenario, where interference between users must be addressed. In order to maintain the same transmit signal power as in the single antenna case, $\mathbf{G}$ is selected such that $\text{tr}(\mathbf{G}\mathbf{G}^{\text{H}}) = N$. One result reported in [5] is that as the number of antennas increase, precoding can be achieved with simple linear operations such as TR. Hence, the constituent TR precoding matrices of $\mathbf{G}$ are represented as

$$\mathbf{G}^{(m)} = \frac{\mathbf{H}^{(m)\text{H}}}{\sqrt{\text{tr}(\mathbf{H}^{(m)\text{H}}\mathbf{H}^{(m)})\frac{M}{N}}}, \tag{21}$$

where m is the FGW antenna index.

The interference power for the UL case shown in (20) also applies to the DL case. The only difference is that the denominator of the noise variance is squared, as is done for the single antenna case.

The capacity results are shown in Fig. 3 and are very similar to Fig. 2 for larger values of M. Note that in Fig. 3, the ideal capacity (solid line) for low antenna counts is higher than the simple detector capacity. This is expected behavior due to the TR precoding. However, as the antenna count increases, the optimal capacity doesn't see the full benefit of the array gain (i.e. 2 times capacity for each doubling of M). In contrast, the simple detector (dashed lines) see the full benefit of the array gain and soon catch up with the optimal capacity. For example, when $M = 32$ and above, the two corresponding curves are virtually indistinguishable.

V. Conclusion

CP-DSSS has tremendous potential as a URLLC or mMTC solution where it would act as a secondary network, using the same spectrum as the primary network but operating at low SNR values. This paper extended the capacity analysis presented in [3] by deriving equations for CP-DSSS capacity using MF detection or TR precoding. When the capacity of the specified detection methods was compared against the capacity of an ideal detector, we found that MF detection was near optimal in the low SNR regime, and TR precoding had performance similar to MF detection. These results also held for the multi-antenna case and over various symbol reduction factors. These impressive results with simple detection or precoding showed that CP-DSSS has great potential to provide URLLC and mMTC solutions with simplified transceiver terminals.

References

[1] A. Aminjavaheri, A. RezazadehReyhani, R. Khalona, H. Moradi and B. Farhang-Boroujeny, "Underlay Control Signaling for Ultra-Reliable Low-Latency IoT Communications," *2018 IEEE International Conference on Communications Workshops (ICC Workshops)*, Kansas City, MO, 2018.

[2] H. Moradi and B. Farhang-Boroujeny, "Underlay scheduling request for ultra-reliable low-latency communications," *IEEE 5G World Forum*, Sept. 30 - Oct. 2, 2019, Dresden, Germany.

[3] B. Kenney, S. Jenkins, A. Majid, H. Moradi, B. Farhang-Boroujeny, "Cyclic Prefix Direct Sequence Spread Spectrum Capacity Analysis," submitted to *International Conference on Communications*, Jun. 2020.

[4] E. Dahlman, S. Parkvall, Johan Skold, "5G NR: The Next Generation Wireless Access Technology," London, United Kingdom: Academic Press, 2018.

[5] J. Hoydis, S. ten Brink and M. Debbah, "Massive MIMO in the UL/DL of Cellular Networks: How Many Antennas Do We Need?," *IEEE Journal on Selected Areas in Communications*, vol. 31, no. 2, pp. 160-171, Feb. 2013.